

Truncated Lévy walk of a nanocluster bound weakly to an atomically flat surface: Crossover from superdiffusion to normal diffusion

Yutaka Maruyama and Junichi Murakami

*Institute for Structural and Engineering Materials (ISEM), National Institute of Advanced Industrial Science and Technology (AIST)
Chubu, 2266-98 Anagahora, Shimo-shidami, Moriyama-ku, Nagoya 463-8560, Japan*

(Received 5 September 2002; published 10 February 2003)

We have demonstrated that the fast stick-slip diffusion of a nanocluster bound weakly to an atomically flat surface such as graphite is a truncated Lévy walk. To do this, a 2 μ s molecular dynamics simulation was performed using a finite two-dimensional Frenkel-Kontolova-type model with Langevin-thermostats. We found that the statistics of jump durations obey a power-law distribution truncated at \sim ns and that the exponent γ of a mean-square displacement ($\sim t^\gamma$) becomes 1 only for $t \geq$ ns. “Short” (200 ns) simulations cannot correctly show the crossover from superdiffusion ($\gamma > 1$) to normal-diffusion ($\gamma = 1$).

DOI: 10.1103/PhysRevB.67.085406

PACS number(s): 61.46.+w, 36.40.Sx, 05.40.Fb

I. INTRODUCTION

Understanding diffusion mechanisms of clusters on surfaces is important from both fundamental and technological points of view.¹ Recently, surface imaging techniques such as transmission electron microscope (TEM) have shown that large clusters with three-dimensional structure (e.g., Sb₂₃₀₀, Au₂₅₀) self-diffuse as a whole on graphite much faster than is expected for uncorrelated thermal motions of atoms.² However, it is difficult to deduce the details of the diffusion mechanism from the images, because the techniques basically image the clusters only in intervals of the diffusion.

To clarify the mechanism, molecular dynamics (MD) simulations have been performed.³⁻⁵ Luedtke and Landman⁴ have shown that a gold cluster on graphite exhibits intermittent “stick-slip” motion accompanied by rotation. The motion intermittently alternated between a oscillatory trapped motion (“stick”) and a sliding jump (“flight” or “slip”) with no apparent influence of the surface. Flight (slip) time and sticking time probability density functions (PDF’s) were found to take power-law distributions rather than Gaussians. This indicates that the total trajectory is possibly characterized as a “Lévy-flight” (LF), or more strictly, as a “Lévy-walk” (LW),⁶ which can involve infinitely long jumps performed with a finite maximal velocity.

The notion of Lévy-flight has widely appeared in physical issues like chaotic diffusion in a rotating fluid flow⁷ and also in nonphysical ones like dynamics of economic indices.⁸ Mathematically, LF obeys a Lévy *stable* distribution (LD) that has power-law tails responsible for *infinite* variance and thus does not fulfill an essential hypothesis needed to apply the central limit theorem (CLT).⁹ In LW, a random-walker visits the same sites of LF. *Instantaneous* jumps (*infinite* velocities) are not allowed and the time to complete each jump of the LW is required. Therefore, variance becomes finite and “superdiffusion” occurs when there are more flights than stickings: mean-square displacements (MSD’s) $\langle [\mathbf{R}(t+q) - \mathbf{R}(q)]^2 \rangle_q = \langle \Delta R^2(t) \rangle$ scale as t^γ with $1 < \gamma < 2$, where $\langle * \rangle_q$ denotes a statistical average over the time q . Luedtke and Landman⁴ concluded from a MSD obtained with a considerably long MD simulation of 90 ns that a gold cluster

(Au₁₄₀) on graphite undergoes a mild superdiffusion ($\gamma = 1.1$).

However, it is doubtful whether the self-diffusive stick-slip motion of the cluster really represents a genuine superdiffusive Lévy walk. This is because cluster-surface systems are not so far from thermal equilibrium as a genuine Lévy walk in an *open* fluid systems⁷ is, where energy is pumped in through rotating. Some fluctuation inherent in the systems not only enhances the jumps but also unavoidably suppresses the occurrence of extremely long jumps responsible for superdiffusion.

The unavoidable suppression of extremely long jumps, or the *truncation* of power-law tails of a LD, makes variance finite. As discussed by Mantegna and Stanley,¹⁰ in such flight, termed *truncated* Lévy flight (TLF), a sum of flights very slowly converges to a Gaussian due to the CLT. We expect therefore that the crossover of diffusivity occurs as follows. In small time scales, since trajectories by *truncated* Lévy walk (TLW) are apparently identical to those by LW and dominated by long-correlated (ballistic) segments, they seemingly give rise to superdiffusion ($\gamma > 1$). On the other hand, in large time scales, almost all trajectories are randomized, exhibiting normal diffusion ($\gamma = 1$). This crossover should be observed by computer simulations if the simulation time is statistically long enough.

The purpose of the present work is to demonstrate that there exists a crossover from the anomalous superdiffusion to the normal diffusion for Lévy-type stick-slip diffusion of a nanocluster on an atomically flat surface-like graphite. So far such a study has not been carried out yet. This is basically due to the difficulty in determining a long-time behavior of the diffusivity that requires very prolonged MD runs with very heavy computational loads (i.e., many degrees of freedom of atoms and complicated many-body interatomic potentials). Here we report an extremely long (2 μ s) MD simulation involving a finite two-dimensional (2D) Frenkel-Kontolova (FK) type model¹¹ with Langevin-thermostats, extended to a three-dimensional cluster on an atomically-flat surface. This model is seemingly oversimplified but can clarify the characteristic diffusion mechanism responsible for the change of diffusivity with increasing time scale.

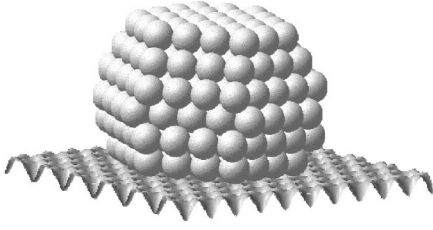


FIG. 1. Snapshot of the model cluster (Au_{245}) on the periodic potential surface (v_{atom}) modeled for graphite.

II. COMPUTATIONAL DETAILS

Diffusive motion of small particles on surfaces is usually believed to be driven by thermal motion of surface atoms. However, for the fast diffusion of clusters bound weakly to atomically flat surfaces, it has been reported by Deltor *et al.*¹² and by Luedtke and Landman⁴ that a static (frozen) substrate can cause a diffusion nearly identical with one caused by fully dynamical substrates. Presumably this is because significant surface lattice deformation, which affects sticking behavior and reduces average diffusion velocity as suggested by Lewis *et al.*,⁵ does not occur due to the weak cluster-surface interactions. (The Au-C interaction of Lewis *et al.*⁵ is about two times stronger than that of Luedtke and Landman.⁴) This suggests that although effects of thermal lattice vibrations in the surfaces cannot be completely neglected, such a surface can be effectively modeled by a static single-atom potential. In the present work, therefore, we consider a model nanocluster not on a computationally heavy atomistic surface but on an analytic periodic potential surface, which mimics Au_{245} on a graphite surface, as shown schematically in Fig. 1.

Since vertical (z) motions of atoms in the present system are probably not so important to the lateral (x - y) motion of the cluster as a whole, the periodic single-atom potential surface is expressed in 2D: $v_{\text{atom}}(x, y)$. On the graphite surface, β carbon atom sites, that have no carbon atoms sitting beneath them in the adjoining graphite sheet, are preferential adsorption sites for metal atoms.¹³ Therefore, v_{atom} is defined not on the honeycomb lattice but on the triangular lattice of the surface (i.e., α carbon atom sites are omitted). For simplicity we assume the three shortest wave vectors' terms of a 2D Fourier series,

$$v_{\text{atom}}(x, y) = E_0 \left[\phi(x, y) = E_0(-2/9) \times \left(\cos \left\{ k \left[x + \frac{y}{\sqrt{3}} \right] \right\} + \cos \left\{ k \frac{2y}{\sqrt{3}} \right\} + \cos \left\{ k \left[x - \frac{y}{\sqrt{3}} \right] \right\} \right) \right].$$

Here k is the length of the shortest wave vectors, related to the lattice constant of graphite ($a_{\text{graphite}} = 2.46 \text{ \AA}$), and the average value of $v_{\text{atom}}(x, y)$ is 0 eV. The amplitude of potential corrugation, E_0 , is thought to be a mere fraction of the binding energy of 0.26 eV/atom for large Au islands on graphite.¹³ Here we set E_0 to 0.06 eV. Thereby, a height of energy barriers for single atoms is about 0.053 eV at a saddle point between potential wells on the triangular lattice.

The model gold cluster is an atomistic three-dimensional nanocrystal of 245 atoms shown in Fig. 1, whose lowermost 37 atoms form a compact hexagon and each interact with the surface [$v_{\text{atom}}(x, y)$] like FK models.¹¹ Interatomic interactions within the cluster are restricted to first nearest neighbors and described not by a harmonic potential used usually for the FK models but by a Lennard-Jones (LJ) (6-12) potential. The depth of the LJ potential well ϵ is set to 0.609 eV, which is derived from the bulk modulus and the interatomic distance ($a_{\text{Au}} = 2.88 \text{ \AA}$) of bulk gold. By similar reasoning for the 2D potential surface, the vertical (z) interatomic distances are always fixed in our simulations.

To take into account the situation that cluster atoms are thermally equilibrated with surface atoms through their *dynamical* interactions, the cluster's lowermost 37 atoms in contact with the potential surface are treated individually by Langevin-dynamics;¹⁴ the dynamical interactions of the cluster atoms with the surface atoms are expressed by random force and friction force in proportion to velocity, both of which are due to thermal motion of atoms and related by the fluctuation-dissipation theorem. On the other hand, the rest upper 208 atoms, which are not in contact with the surface, are treated by Newtonian-dynamics using a velocity Verlet algorithm. The time step Δt is 5 fs. The Langevin damping-time constant, $1/\xi$, is set to 100 ps.¹⁵ By 37 Langevin-thermostats, the atoms in the cluster are thermally equilibrated at a given temperature T .

III. RESULTS AND DISCUSSION

We first show in Fig. 2(a) an x - y trajectory of the cluster's center-of-mass for ~ 1.5 ns at 500 K, and in Fig. 2(b), its x , y , and rotational (θ) components. In Fig. 2(a) we find that the cluster stick-slip-diffuses from the site A to the site B without apparent influence of the surface morphology (open circles). The diagonal lines in Fig. 2(b) represent flights of the cluster. The oscillations about horizontal lines on right and left sides are stickings at the sites A and B. Some of the sharply curved parts in the slip-motion are also due to a sticking event (see the criterion given below for classifying sticking events). The periods τ of x , y , and θ oscillations shown on the right-hand side of Fig. 2(b) are 23, 24, and 16 ps, respectively, and consistent with the corresponding values of $\tau \sim 20$ ps reported by the previous studies.^{4,5} This stick-slip motion is basically identical to that obtained by more realistic modelings, which demonstrates the validity of the present simplified model.

Figure 3(a) shows a 2000 ns ($= 2 \mu\text{s}$) x - y trajectory, and Figs. 3(b)-3(e) its x component on four different spatio-temporal scales. Compared to the previous studies, the simulation time of the present study is one order of magnitude longer. (Luedtke and Landman⁴ performed a 90 ns simulation and Lewis *et al.*,⁵ a 125 ns simulation, for static substrates.) From Figs. 3(c)-3(e), we find self-similar stick-slip behavior, characterized by horizontal lines (stickings) and diagonal lines (flights), which is also reported in the previous studies.^{4,5} On the other hand, Fig. 3(b) as well as Fig. 3(a) show the behavior on the time scale one order of magnitude larger than the previous studies. It is seen from the figures

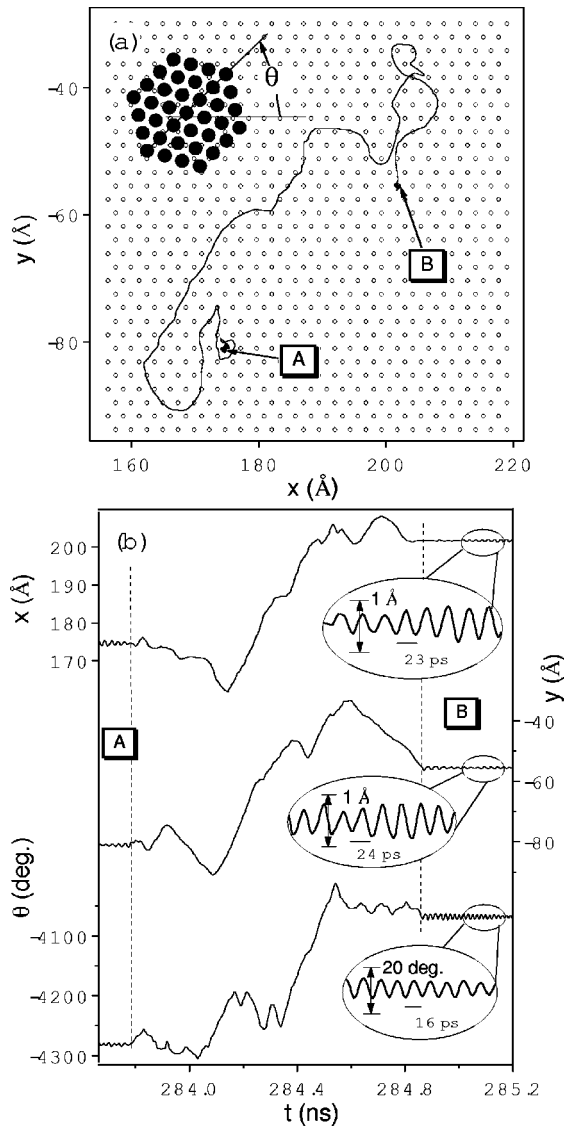


FIG. 2. (a) 1.5 ns x - y trajectory of the cluster's center-of-mass at 500 K. The small open circles (\circ) represent the minimum potential energy sites (β -sites) in the periodic potential surface. The large closed circles represent the lowermost 37 atoms of the cluster (\bullet). θ is the cluster's angle of rotation relative to the surface lattice. (b) The variations in x , y , and θ as a function of time.

that the characteristic stick-slip behavior is almost lost. In other words, on large spatio-temporal scales, the fluctuation of the x component becomes close to an ordinary Brownian motion characterized by a Gaussian, which implies a crossover from a Lévy-walk to a normal random walk.

Before going to the discussion about the MSD of the cluster, we examine whether the statistics of the stick-slip behavior have power-law nature indicative of a Lévy-walk. To calculate the flight time PDF, $p_f(t)$, and the sticking time PDF, $p_s(t)$, we divide the whole trajectory into a succession of sticking and flight intervals as in Refs. 14 and 4; for every 2 ps distance $d(t_i) = |\mathbf{R}(t_i - \tau/2) - \mathbf{R}(t_i + \tau/2)|$ is computed, and if $d(t_i) < d_c$, the event is then identified as a sticking one. In the analysis, the sticking period (τ) of 20 ps, and the sticking amplitude (d_c) of 0.6 Å, the same values as those of

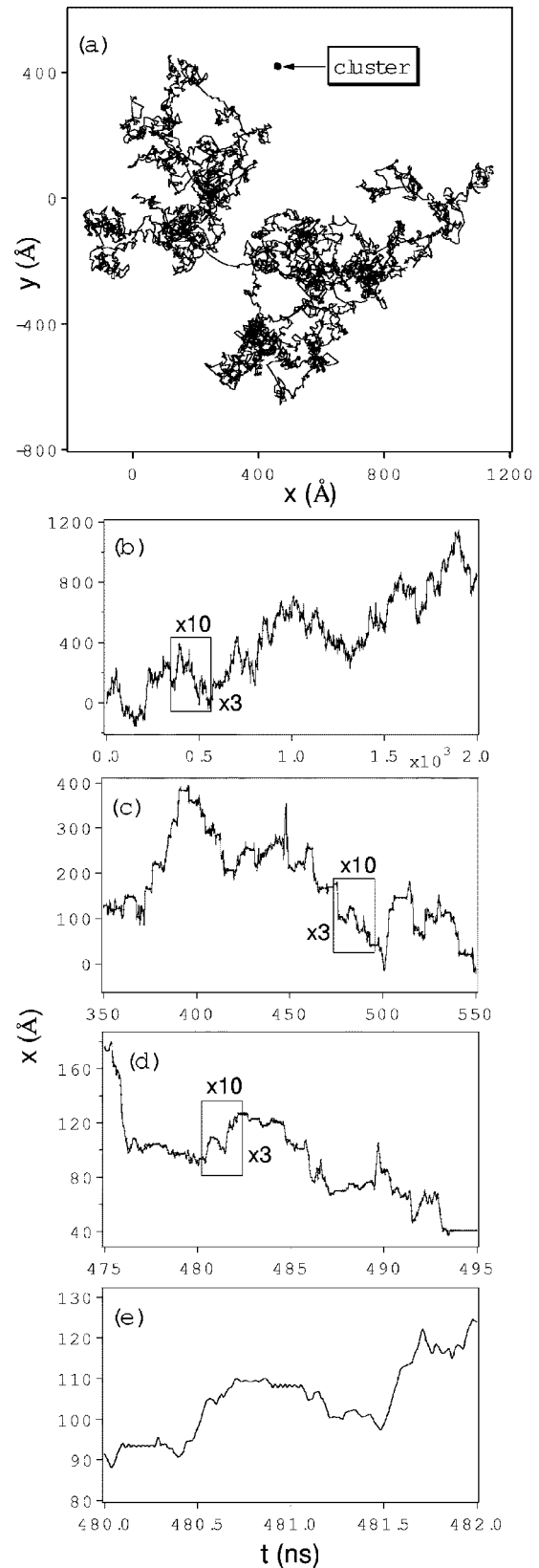


FIG. 3. (a) 2 μ s x - y trajectory of the cluster's center-of-mass at 500 K. The small closed dot represents the size of the cluster. (b)-(e) The x component of the trajectory in four different spatio-temporal scales. The area in the small rectangle in (b) is expanded to a full scale in (c), and the like from (c) to (d) and from (d) to (e).

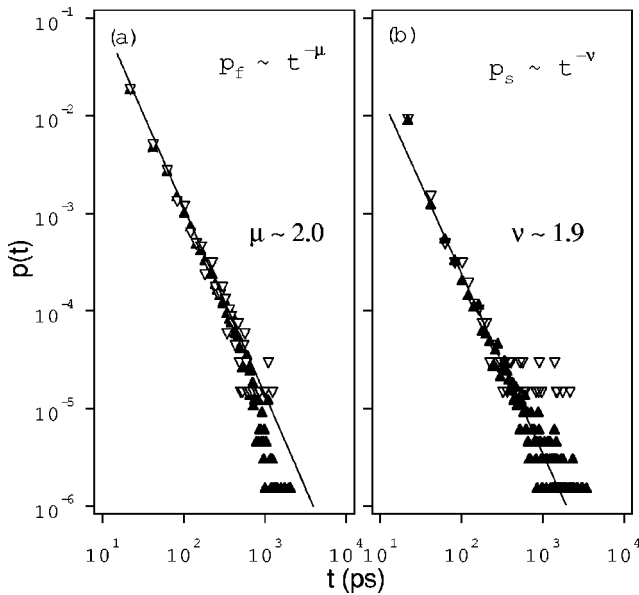


FIG. 4. Histograms of flight times $p_f(t)$ (a) and sticking times $p_s(t)$ (b), calculated from the $2 \mu\text{s}$ MD simulation (closed triangles) and its portion of 200 ns (open inverted triangles). Histogram bin width (Δt) is 20 ps (see text). The flight times obey a power-law probability density function $\sim t^{-\mu}$ with $\mu \sim 2.0$, and sticking times $\sim t^{-\nu}$ with $\nu \sim 1.9$.

Ref. 4 are used. Flight events are then simply the intervals between the stickings. The PDF's are determined from histograms of the flight and stick durations. The histograms are normalized according to $\sum_n p(t_n) \Delta t = 1$, where duration t is rounded to t_n every 20 ps (= histogram bin width $\Delta t = \tau$) because of the uncertainty between sticking and flight events below τ .

We show in Fig. 4 the histograms of the flight times (a) and the sticking times (b), obtained from the full dataset of the 2000 ns x - y stick-slip diffusion (closed triangles) and its portion of 200 ns (open inverted triangles). Each figure indicates a power-law relation for both the two datasets, demonstrating the temporal self-similarity of the stick-slip behavior in Figs. 3(c)–3(e): $p_f(t) \sim t^{-\mu}$ with $\mu \sim 2.0$, and $p_s(t) \sim t^{-\nu}$ with $\nu \sim 1.9$. These exponents are a little different from the results ($\mu \sim 2.3$ and $\nu \sim 2.1$) in Ref. 4 probably because of differences in the size of the cluster and the interatomic interactions. However, the overall reproduction of the characteristic stick-slip diffusion is very good. This indicates either the validity of our simplified model or the presence of some universal mechanism (such as, for example, self-organized criticality¹⁶) which is independent of details of models.

As seen in Fig. 3(e), the slopes of the diagonal lines are always almost the same. This indicates that the flight speeds are almost the same and that they are constant during the flights. This allows us to suppose that the flight duration is in proportion to jump length “ ℓ ,” i.e., the power-law relation of $p_f(t)$ indeed indicates a power-law tail of a LD $p_f(\ell)$ with no typical jump length, or characteristics of LW.

It should be noted that, for $t > \text{ns}$, there is a drop-off in the flight time histogram obtained from the 2000 ns dataset. The drop-off, a transition from power-law decay to much

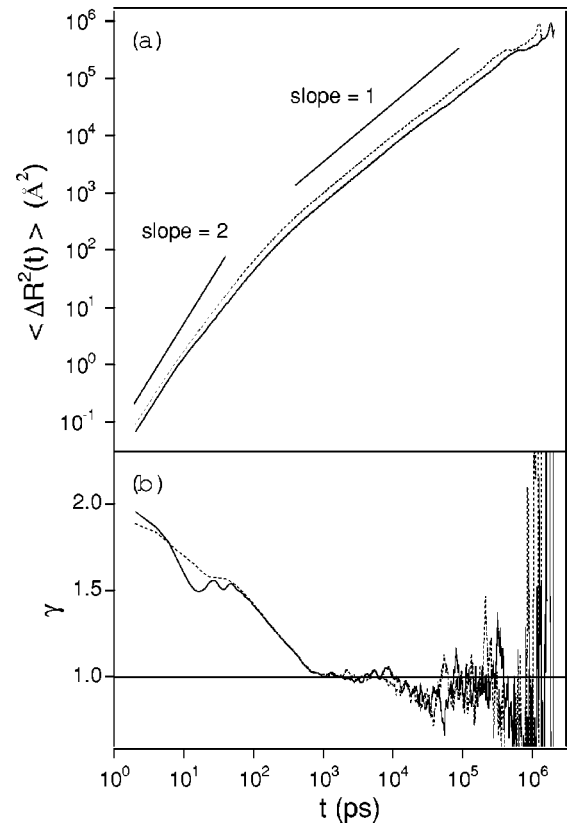


FIG. 5. (a) Log-log plots of MSD's for the Lévy-type cluster surface diffusion at 500 K and (b) the slopes, γ , of the plots. The solid curve was derived from the full dataset of the $2 \mu\text{s}$ x - y stick-slip trajectory in Fig. 3(a) and the dotted curve from the reduced dataset consisting only of flight events in the full dataset. The solid lines with slopes of 2 (ballistic) and 1 (Brownian-type) in (a) are guides to the eyes.

faster (exponential) decay, is indicative of truncation of tails of the LD. In self-diffusive cluster-surface systems, infinitely long(-lived) jumps, which violate equipartition of energy and thermalization with surfaces, are unrealistic and unavoidably interfered by some fluctuation inherent in the systems and decay, which is not the case for *open* systems⁷ where energy is pumped in.

There seems to be no drop-off in the sticking time histograms within the present simulation time of $2 \mu\text{s}$. This may imply that the sticking time PDF can have an infinitely long tail, although the statistics could be still insufficient to clarify the point.

We show in Fig. 5(a) a log-log plot of the MSD calculated from the full dataset of the $2 \mu\text{s}$ stick-slip trajectory in Fig. 3(a), and in Fig. 5(b) its slope, $\gamma = d \log[\langle \mathbf{R}(t+q) - \mathbf{R}(q) \rangle_q^2] / d \log t$. When the slope is 2, it represents a ballistic motion, and the slope of 1 corresponds to an ordinary Brownian-type motion. (The increase in the fluctuation of γ for $t \gtrsim 10^4$ ps reflects the fact that the data are less accurate at large t because the number of samples for a statistical average over q decreases with t .) From the figures, we can see a crossover from superdiffusion ($1 < \gamma < 2$) corresponding to the Lévy-type power-law flight PDF for $t \lesssim \text{ns}$ to normal diffusion ($\gamma = 1$) due to the truncation of the PDF for t

\geq ns. This is consistent with a visual inspection of the trajectory for 1.5 ns in Fig. 2(a): In time scales smaller than a maximum flight duration of \sim ns, TLW is seemingly identical to LW, and some trajectories are partially randomized while others are dominated by a long-correlated (linear) excursion, which results in superdiffusion ($\gamma > 1$). On the other hand, in time scales larger than the maximum flight duration, almost all trajectories are randomized and this gives rise to the crossover to normal diffusion ($\gamma = 1$). Statistically good convergence to $\gamma = 1$ requires long MD simulations. We observed that small datasets of ~ 100 ns can sometimes exhibit no crossover to normal diffusion because of the lack of statistics.

The diffusion coefficient $D(=\langle \Delta R^2(t) \rangle / 4t)$ of the cluster is estimated to be 1.75×10^{-5} cm²/s from the linear part (10^3 ps $< t < 10^4$ ps) in the MSD. This value is about ten orders of magnitude larger than those for other cluster-surface systems such as compact Ir clusters on atomically flat Ir surfaces.¹⁷ However, the value of D is three orders of magnitude smaller than estimated at 500 K from the density of self-similar ramified-cluster-islands measured by TEM.² As discussed by Lewis *et al.*,⁵ this huge discrepancy is probably mainly due to errors in the estimation of cluster deposition flux and in “deposition-diffusion-aggregation” (DDA) model’s assumptions to analyze experiments.² Using realistic many-body potentials, Lewis *et al.*⁵ reported 3.71 and 1.09×10^{-5} cm²/s for dynamic and frozen substrates, respectively (γ were estimated to be 0.9–1.2), which strongly supports our result.

As was noted by Luedtke and Landman⁴ and references therein, it is known that when mathematically genuine LW’s with infinite variance coexist with stickings, diffusivity is either anomalous (super- : $1 < \gamma < 2$; sub- : $0 < \gamma < 1$) diffusion or normal diffusion ($\gamma = 1$) depending on statistics of

the stickings (ν) as well as the LW’s (μ). On the other hand, the effect of stickings on the crossover to normal diffusion due to being a TLW is unclear. To assess the effect, we made a reduced ($\sim 68\%$) dataset which consists only of flight events [for $d(t_i) > d_c$] out of the full dataset of 2000 ns to calculate a MSD and its γ . The results (dotted lines) are shown in Figs. 5(a) and 5(b). The upward constant shift from the solid line in Fig. 5(a) is due to the difference in average diffusion velocity. Figure 5(b) shows that the solid and dotted lines almost overlap for $t > 10^2$ ps and this indicates that the crossover originates only from the truncation of flight duration. From the discrepancy for $t < 10^2$ ps, it can be seen that the oscillation around a few tens of ps is due to long oscillatory sticking motion.

IV. CONCLUSION

To clarify long-time asymptotic behavior of Lévy-type stick-slip diffusion of a nanocluster bound weakly to an atomically flat surface such as graphite, we have presented a finite 2D Frenkel-Kontolova-type model with Langevin-thermostats and performed an extremely long 2 μ s molecular dynamics simulation. We have found that the statistics of jump (flight) duration take a Lévy-type power-law distribution truncated at about ns, which results in crossover from Lévy-type superdiffusion for $t \lesssim$ ns to normal diffusion for $t \gtrsim$ ns. We also found that that for relatively “short” ($t = 200$ ns) simulations the truncation cannot be obtained because of lack of statistical reliability. This indicates that the correct long-time behavior probably cannot be obtained from short simulations.

ACKNOWLEDGMENTS

We thank Y. Tai and W. Yamaguchi for fruitful discussions and comments.

¹P. Jensen, *Rev. Mod. Phys.* **71**, 1695 (1999), and references therein.

²L. Bardotti *et al.*, *Surf. Sci.* **367**, 276 (1996), and references therein.

³Y. Maruyama, J. Murakami, and S. Tanemura, *Rep. Nat. Indust. Res. Inst. of Nagoya* **46**, 445 (1997).

⁴W. D. Luedtke and U. Landman, *Phys. Rev. Lett.* **82**, 3835 (1999).

⁵L. J. Lewis, P. Jensen, N. Combe, and J-L. Barrat, *Phys. Rev. B* **61**, 16084 (2000).

⁶M. F. Shlesinger, G. M. Zaslavsky, and J. Klafter, *Nature (London)* **363**, 31 (1993), and references therein.

⁷T. H. Solomon, E. R. Weeks, and H. L. Swinney, *Phys. Rev. Lett.* **71**, 3975 (1993).

⁸R. N. Mantegna and H. E. Stanley, *Nature (London)* **376**, 46 (1995).

⁹N. G. van Kampen, *Stochastic Processes in Physics and Chemistry: Revised and Enlarged Edition* (N-H. Personal Library, Amsterdam, 1992).

sterdam, 1992).

¹⁰R. N. Mantegna and H. E. Stanley, *Phys. Rev. Lett.* **73**, 2946 (1994).

¹¹The classical standard Frenkel-Kontorova model represents an infinitely long one-dimensional chain of particles harmonically coupled with their neighbors and subjected to an incommensurate sinusoidal potential.

¹²P. Deltour, J-L. Barrat, and P. Jensen, *Phys. Rev. Lett.* **78**, 4597 (1997).

¹³E. Ganz, K. Sattler, and J. Clarke, *Surf. Sci.* **219**, 33 (1989).

¹⁴M. P. Allen and D. J. Tildesley, *Computer Simulation of Liquids* (Oxford University Press, Oxford, 1987).

¹⁵We observed that the results do not significantly change for $1/\xi = 10, 50, 100, 500$, and ∞ ps. Here $\xi = 1/\infty = 0$ corresponds to a *microcanonical* situation with no Langevin-thermostat.

¹⁶P. Bak, *How Nature Works* (Springer-Verlag, New York, 1996).

¹⁷S. C. Wang, U. Kurpick, and G. Ehrlich, *Phys. Rev. Lett.* **81**, 4923 (1998).